Analysis of the conjugate transient natural convection–conduction heat transfer of a fin array in a cavity

T.-M. Chen and C.-K. Chen
Department of Mechanical Engineering, National Cheng Kung University, Tainan, Taiwan, 70101, Republic of China

This article is concerned with the conjugate transient natural convection–conduction heat transfer for finned packages in a cavity. The situation is commonly found in the cooling of very large scalar integration (VLSI) electronic packages in a closed space. The present study uses a numerical integration technique with a cubic spline to solve the conjugate coupled nonlinear partial differential equations. Results are obtained for a range of values of Prandtl and Rayleigh numbers and the fin and fluid thermal diffusivity ratio. The transient and steady-state phenomena of the velocity and temperature field and average Nusselt numbers on the hot surface, cold surface, and fin are presented.

Keywords: heat transfer; transient natural convection–conduction; cavity flow

Introduction

Conjugate convection and conduction problems for a vertical plate fin have been analyzed by Sparrow and Acharya[1] and Huang and Chen.[2,3] But these studies were restricted to steady-state heat transfer and boundary-layer flow field. A rectangular cell enclosed by vertical plate fins under isothermal conditions is used in many engineering applications, as for example, in the cooling of VLSI electronic packages in a closed cavity or solar energy collectors for storing solar energy. Apparently, no studies report the use of conjugate and conduction theory to analyze the case. In the present investigation, attention is focused on the analysis of two-dimensional (2-D) transient natural convection head transfer in a rectangular cell enclosed by vertical plate fins and hot and cold surfaces, which are horizontal and isothermal.

Because the temperature of the fin is unknown (it is affected by the heat transfer coefficient), the heat transfer coefficient also depends on the cavity flow. Hence it is necessary to solve the conjugate convection and conduction problem, which can be separated into two parts: (1) the conservation equations of the laminar free convection 2-D Navier–Stokes equations flow field; and (2) the energy equations of the fin. Owing to the highly nonlinear nature of the problem, an exact solution is not feasible. Therefore the spline alternating direction implicit (SADI) method[4] is utilized to solve the nondimensional equations.

The boundary condition at the fin–fluid interface must satisfy the conjugate conditions (the energy fluxes flowing out of the fin equals that flowing into the fluid and the temperature in the surface of the fin equals that in the surface of the fluid). Thus we assume that the plate fin is 2-D.

With regard to transient heat transfer, at each time step, the assumed plate fin temperature distributions serve as boundary conditions for the 2-D Navier–Stokes equations. The solutions of the instantaneous temperature distributions of the fluid from the Navier–Stokes equations are resubstituted into the conjugate conditions of the fin energy equation in search of the new fin temperature distributions. These new temperature distributions are then imposed as the surface boundary conditions for the Navier–Stokes equations. The solutions are used to satisfy the updated conjugate conditions until the maximum difference of temperature between successive iterations $<10^{-4}$. Then, the next time step solutions are calculated.

Numerical results are presented for the average Nusselt number and fin temperature distribution, the average Nusselt number for hot and cold surfaces, and the fluid field temperature and velocity distributions.

Address reprint requests to Dr. Cha'o-Kuang Chen at the Department of Mechanical Engineering, National Cheng Kung University, Tainan, Taiwan, 70101, Republic of China.

Received 16 October 1989; accepted 3 September 1990

Mathematical analysis

Governing equation

Consider a rectangular cell enclosed by vertical plate fins, having hot and cold surfaces. The plate fin thickness is 2δ and its length is L. The cell width is L'. The coordinates normal and parallel to the fin surface are designated x and y, respectively. The coordinate system is shown in Figure 1. The following assumptions are made to obtain the conservation equations.

(1) The Boussinesq approximation is used for the fluid.
(2) The fluid is Newtonian.
(3) The thermophysical properties, such as viscosity, thermal conductivity, and thermal expansion coefficient, are constant.
(4) The flow is laminar, incompressible, and 2-D.
(5) The viscous dissipation effect is negligible.

The governing equations for fluid vorticity and stream function are

$$\frac{\partial^2\psi}{\partial x^2}+\frac{\partial^2\psi}{\partial y^2}=-\omega \tag{1}$$

$$\frac{\partial\omega}{\partial t}+u\frac{\partial\omega}{\partial x}+v\frac{\partial\omega}{\partial y}=\nu\left(\frac{\partial^2\omega}{\partial x^2}+\frac{\partial^2\omega}{\partial y^2}\right)+\beta g\frac{\partial T}{\partial x} \tag{2}$$

$$\frac{\partial T}{\partial t}+u\frac{\partial T}{\partial x}+v\frac{\partial T}{\partial y}=\alpha\left(\frac{\partial^2 T}{\partial x^2}+\frac{\partial^2 T}{\partial y^2}\right) \tag{3}$$

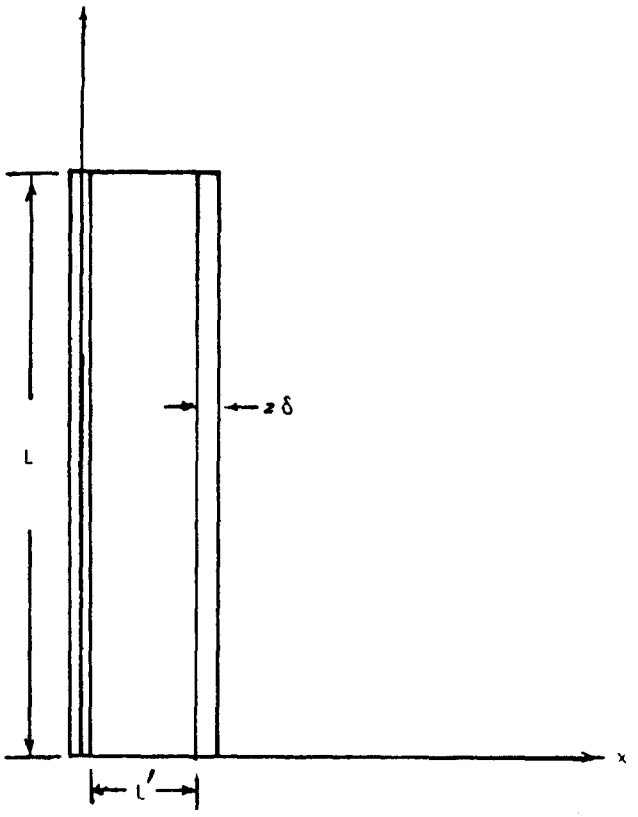

Figure 1 The cell x and y coordinates

where u and v are the x and y direction velocity components, respectively; T is fluid temperature; t is time; and the other symbols are as given in the Notation.

The initial and boundary conditions are

$$\begin{aligned}
&t\le 0 \quad u=v=0 \quad T=T_0 && \text{for all } x, y\\
&t>0 \quad u=v=0 \quad T=T_w(y,t) && \text{for } x=\delta,\ 0\le y\le L\\
&\qquad u=v=0 \quad T=T_w(y,t) && \text{for } x=L'+\delta_1,\ 0\le y\le L\\
&\qquad u=v=0 \quad T=T_0 && \text{for } y=0,\ \delta\le x\le L'+\delta\\
&\qquad u=v=0 \quad T=T_0+\Delta T && \text{for } y=L,\ \delta\le x\le L'+\delta
\end{aligned} \tag{4}$$

where $T_w(y, t)$ is the wall temperature to be determined. The no-slip condition is satisfied at the wall.

The plate fin equation is given by

$$\frac{\partial T_f}{\partial t}=\alpha_f\left(\frac{\partial^2 T_f}{\partial x^2}+\frac{\partial^2 T_f}{\partial y^2}\right) \tag{5}$$

where T_f is the fin temperature and α_f is the fin thermal diffusivity. The associated initial and boundary conditions are

$$\begin{aligned}
&t\le 0 \quad T_f=T_0 && \text{for all } x, y\\
&\qquad \frac{\partial T_f}{\partial x}=0 && \text{for all } x=0,\ 0\le y\le L\\
&\qquad T_f=T_0 && \text{for all } y=0,\ 0\le x\le \delta\\
&\qquad T_f=T_0+\Delta T && \text{for all } y=L,\ 0\le x\le \delta
\end{aligned} \tag{6}$$

Of particular interest is the thermal coupling between fin and fluid. The basic coupling is expressed by the requirement that

Notation

g	Gravitational acceleration
h	Heat transfer coefficient
k	Fluid heat conductivity
k_f	Fin heat conductivity
L	Length of the plate fin
L'	Width of the cavity
$L_{i,j}$, $M_{i,j}$	Spline second derivative in the y and x direction, respectively
$l_{i,j}$, $m_{i,j}$	Spline first derivative in the y and x direction, respectively
Nu_x	Local Nusselt number of the fluid in the x direction, $\frac{h_x L}{k}$
$\overline{\mathrm{Nu}}_x$	Average Nusselt number of the fluid in the x direction, $\frac{\bar{h}_x L'}{k}$
Nu_{fx}	Local Nusselt number of the fin in the x direction, $\frac{h_{fx} L}{k_f}$
Nu_y	Local Nusselt number of the fluid in the y direction, $\frac{h_y L}{k}$
$\overline{\mathrm{Nu}}_y$	Average Nusselt number of the fluid in the y direction, $\frac{\bar{h}_y L}{k}$
Pr	Prandtl number, $\frac{\nu}{\alpha}$
Ra	Rayleigh number, $\frac{g\beta(\Delta T)L^3}{\nu\alpha}$
t	Time
Δt	Time step
T	Fluid temperature
T_f	Fin temperature
ΔT	Overall temperature difference
u, v	Velocity components in the x and y directions, respectively
x, y	Spatial coordinate normal to and along the plate fin, respectively
Greek symbols	
α	Thermal diffusivity of fluid
α_f	Thermal diffusivity of fin
β	Volumetric coefficient of thermal expansion
δ	Half-thickness of the plate fin
ρ	Fluid density
ν	Kinematic viscosity
τ	Fictitious time
$\Delta\tau$	Fictitious time step
ψ	Stream function
ω	Vorticity
Superscripts	
*	Dimensionless parameter
n	Index of time step Δt
s	Index of fictitious time step $\Delta\tau$
Subscripts	
i, j	Index of nodal points in the x and y direction, respectively
w	Condition at the wall
f	Property of plate fin

the temperature and heat flux are continuous at the fin–fluid interface; that is,

$$T_f(y,t)=T_w(y,t)$$
$$-k_f\frac{\partial T_f}{\partial x}=-k\frac{\partial T}{\partial x} \qquad \text{for } t>0,\ x=\delta,\ x=L'+\delta, \text{ and } 0\le y\le L \tag{7}$$

The conservation equations can be cast into dimensionless form by introducing the length of the plate fin as the reference length, appropriate stretched coordinates and normalized velocities, temperature, vorticity, and stream function and defined as:

$$x^*=\frac{x}{L} \quad y^*=\frac{y}{L} \quad \omega^*=\frac{\omega L^2}{\alpha} \quad \psi^*=\frac{\psi}{\alpha} \quad k^*=\frac{k_f}{k}$$
$$\alpha^*=\frac{\alpha_f}{\alpha} \quad u^*=\frac{uL}{\alpha} \quad v^*=\frac{vL}{\alpha} \quad T^*=\frac{T-T_0}{\Delta T} \tag{8}$$
$$T_f^*=\frac{T_f-T_0}{\Delta T} \quad t^*=\frac{t\alpha}{L^2} \quad \mathrm{Ra}=\frac{g\beta(\Delta T)L^3}{\nu\alpha} \quad \mathrm{Pr}=\frac{\nu}{\alpha}$$
$$\delta^*=\frac{\delta}{L} \quad L'^*=\frac{L'}{L} \quad T_w^*=\frac{T_w-T_0}{\Delta T}$$

Equations 1–7 may be reduced to the following nondimensional forms (for simplicity, we omitted the *):

$$\frac{\partial^2\psi}{\partial x^2}+\frac{\partial^2\psi}{\partial y^2}=-\omega \tag{9}$$
$$\frac{\partial\omega}{\partial t}+u\frac{\partial\omega}{\partial x}+v\frac{\partial\omega}{\partial y}=\mathrm{Pr}\left(\frac{\partial^2\omega}{\partial x^2}+\frac{\partial^2\omega}{\partial y^2}\right)+\mathrm{RaPr}\frac{\partial T}{\partial x} \tag{10}$$
$$\frac{\partial T}{\partial t}+u\frac{\partial T}{\partial x}+v\frac{\partial T}{\partial y}=\left(\frac{\partial^2 T}{\partial x^2}+\frac{\partial^2 T}{\partial y^2}\right) \tag{11}$$
$$\frac{\partial T_f}{\partial t}=\alpha\left(\frac{\partial^2 T_f}{\partial x^2}+\frac{\partial^2 T_f}{\partial y^2}\right) \tag{12}$$

The corresponding initial and boundary conditions of the fluid are

$$\begin{array}{llll} t\le 0 & u=v=0 & T=0 & \text{for all } x, y \\ t>0 & u=v=0 & T=T_w(y,t) & \text{for } x=\delta,\ 0\le y\le 1 \\ & u=v=0 & T=T_w(y,t) & \text{for } x=L'+\delta,\ 0\le y\le 1 \\ & u=v=0 & T=0 & \text{for } y=0,\ \delta\le x\le L'+\delta \\ & u=v=0 & T=1 & \text{for } y=1,\ \delta\le x\le L'+\delta \end{array} \tag{13}$$

The corresponding initial and boundary conditions of the fin are

$$\begin{array}{ll} t\le 0 & T_f=0 \quad \text{for all } x, y \\ & \dfrac{\partial T_f}{\partial x}=0 \quad \text{for all } x=0,\ 0\le y\le 1 \\ & T_f=0 \quad \text{for all } y=0,\ 0\le x\le\delta \\ & T_f=1 \quad \text{for all } y=1,\ 0\le x\le\delta \end{array} \tag{14}$$

The corresponding fin–fluid interface conditions are

$$T_f(y,t)=T_w(y,t)$$
$$-k\frac{\partial T_f}{\partial x}=-\frac{\partial T}{\partial x} \qquad \text{for } t>0,\ x=\delta,\ x=L'+\delta, \text{ and } 0\le y\le 1 \tag{15}$$

From Equations 9–15 it is evident that the important parameters of the problem include the Prandtl (Pr) and Raleigh (Ra) numbers and the ratio of fin and fluid thermal diffusivity (α) and the thermal conductivity (k). The physical quantities of interest include the local and average Nusselt numbers. These values are then expressed in dimensionless form:

$$\mathrm{Nu}_x=-\left(\frac{\partial T}{\partial y}\right)_w \tag{16}$$
$$\mathrm{Nu}_y=-\left(\frac{\partial T}{\partial x}\right)_w \tag{17}$$
$$\overline{\mathrm{Nu}}_x=-\frac{1}{L'}\int_0^{L'}\left(\frac{\partial T}{\partial y}\right)dx \tag{18}$$
$$\overline{\mathrm{Nu}}_y=-\int_0^1\left(\frac{\partial T}{\partial x}\right)dy \tag{19}$$
$$\mathrm{Nu}_{fx}=-\left(\frac{\partial T_f}{\partial y}\right)_w \tag{20}$$

In this study we obtained Prandtl numbers of 0.711 and 7.0, Rayleigh numbers of 8.317×10^3 and 8.317×10^5, and fin–fluid thermal diffusivity ratios of 4.36223 and 436.223.

Numerical solution

The conjugate coupled nonlinear partial differential Equations 9–12, subjects to Equations 13–15, were solved by a numerical technique using cubic splines. The principal advantages of using a cubic spline procedure are the following:

(1) The requirement of a uniform mesh is not necessary. For a uniform mesh, however, the spline approximation is fourth-order accurate for the first derivative but is only third-order accurate for a nonuniform grid. The second derivative is approximated to second order for the uniform as well as the nonuniform grid.
(2) The value of first or second derivatives may be evaluated directly, so boundary conditions containing derivatives may be directly incorporated into the solution procedure.
(3) The governing matrix system obtained with the implicit formulation is always tridiagonal, thus facilitating the inversion procedure. The matrix system obtained may be reduced to a scalar set of equations that either contain values of the function itself, its first derivative, or its second derivative at the node points while maintaining a tridiagonal formulation.

For solving partial differential equations with two space dimensions such that

$$u_t=f(u, u_x, u_y, u_{xx}, u_{yy}) \tag{21}$$

an SADI formulation is utilized. The two-step procedure, with quasi-linearization or some other iterative process used for nonlinear terms, is

- Step 1:

$$u_{i,j}^{n+1/2}=u_{i,j}^n+\frac{\Delta t}{2}f(u_{i,j}^{n+1/2}, m_{i,j}^{n+1/2}, M_{i,j}^{n+1/2}, l_{i,j}^n, L_{i,j}^n) \tag{22a}$$

- Step 2:

$$u_{i,j}^{n+1}=u_{i,j}^{n+1/2}+\frac{\Delta t}{2}f(u_{i,j}^{n+1/2}, m_{i,j}^{n+1/2}, M_{i,j}^{n+1/2}, l_{i,j}^{n+1}, L_{i,j}^{n+1}) \tag{22b}$$

where $l_{i,j}$ and $L_{i,j}$ are the spline approximations to $(u_y)_{i,j}$ and $(u_{yy})_{i,j}$, respectively.

Solutions are obtained by the iterative SADI procedure. The

SADI system representing Equations 9–12 is given in two steps for the stream function, vorticity, and energy equations. The stream function is

$$\psi_{i,j}^{n+1,s+1/2}=\psi_{i,j}^{n+1,s}+\frac{\Delta\tau}{2}\left[(L_{i,j}^{\psi})^{n+1,s+1/2}+(M_{i,j}^{\psi})^{n+1,s}+\omega_{i,j}^{n+1}\right] \tag{23a}$$

$$\psi_{i,j}^{n+1,s+1}=\psi_{i,j}^{n+1,s+1/2}+\frac{\Delta\tau}{2}\left[(L_{i,j}^{\psi})^{n+1,s+1/2}+(M_{i,j}^{\psi})^{n+1,s+1}+\omega_{i,j}^{n+1}\right] \tag{23b}$$

where $\Delta\tau$ is a fictitious time step and $\tau=s\Delta\tau$. Solutions to Equation 9 are obtained as the steady-state limit ($\tau\to\infty$) of Equations 23. The notation $L_{i,j}^{A}$ and $M_{i,j}^{A}$ denote the spline approximation to $\partial^2 A/\partial y^2$ and $\partial^2 A/\partial x^2$, respectively, with the superscript ψ implying that $A=\psi$. First derivatives $\psi_y=u$ and $\psi_x=-v$ are represented by $l_{i,j}^{\psi}$ and $m_{i,j}^{\psi}$, respectively. The vorticity equation is

$$\omega_{i,j}^{n+1/2}=\omega_{i,j}^{n}+\frac{\Delta t}{2}\left[-l_{i,j}^{\bar{\psi}}(m_{i,j}^{\omega})^{n}+m_{i,j}^{\bar{\psi}}(l_{i,j}^{\omega})^{n+1/2}+\mathrm{Pr}(L_{i,j}^{\omega})^{n+1/2}+\mathrm{Pr}(M_{i,j}^{\omega})^{n}+\mathrm{RaPr}\left(\frac{\partial T}{\partial x}\right)^{n+1}\right] \tag{24a}$$

$$\omega_{i,j}^{n+1}=\omega_{i,j}^{n+1/2}+\frac{\Delta t}{2}\left[-l_{i,j}^{\bar{\psi}}(m_{i,j}^{\omega})^{n+1}+m_{i,j}^{\bar{\psi}}(l_{i,j}^{\omega})^{n+1/2}+\mathrm{Pr}(L_{i,j}^{\omega})^{n+1/2}+\mathrm{Pr}(M_{i,j}^{\omega})^{n+1}+\mathrm{RaPr}\left(\frac{\partial T}{\partial x}\right)^{n+1}\right] \tag{24b}$$

The bar over superscript ψ in the spline derivatives denotes an average of values at time steps n and $n+1$. Superscript ω denotes ω spline derivatives. The energy equation is

$$T_{i,j}^{n+1/2}=T_{i,j}^{n}+\frac{\Delta t}{2}\left[-l_{i,j}^{\bar{\psi}}(m_{i,j}^{T})^{n}+m_{i,j}^{\bar{\psi}}(l_{i,j}^{T})^{n+1/2}+(L_{i,j}^{T})^{n+1/2}+(M_{i,j}^{T})^{n}\right] \tag{25a}$$

$$T_{i,j}^{n+1}=T_{i,j}^{n+1/2}+\frac{\Delta t}{2}\left[-l_{i,j}^{\bar{\psi}}(m_{i,j}^{T})^{n+1}+m_{i,j}^{\bar{\psi}}(l_{i,j}^{T})^{n+1/2}+(L_{i,j}^{T})^{n+1/2}+(M_{i,j}^{T})^{n+1}\right] \tag{25b}$$

The heat conduction equation is

$$T_{fi,j}^{n+1/2}=T_{fi,j}^{n}+\frac{\Delta t\alpha}{2}\left[(L_{i,j}^{T_f})^{n+1/2}+(M_{i,j}^{T_f})^{n}\right] \tag{26a}$$

$$T_{fi,j}^{n+1}=T_{fi,j}^{n+1/2}+\frac{\Delta t\alpha}{2}\left[(L_{i,j}^{T_f})^{n+1/2}+(M_{i,j}^{T_f})^{n+1}\right] \tag{26b}$$

In this study, we assumed that the steady-state condition existed when the relative maximum change of variables u, v, T, and T_f at every node between two time steps was less than 10^{-4}; i.e., where ϕ represents u, v, T, and T_f,

$$\frac{\|\phi_{i,j}^{n+1}-\phi_{i,j}^{n}\|_{\max}}{\|\phi_{i,j}^{n+1}\|_{\max}}<10^{-4}$$

Results and discussion

Numerical results were obtained for isothermal surfaces, with cavity width $L'^{*}=0.2$, plate fin half-thickness $\delta^{*}=0.02$, Pr of 0.711 and 7.0, Ra of 8.317×10^{3} and 8.317×10^{5}, and fin–fluid thermal diffusivity (α^{*}) ratios of 4.36223 and 436.223.

Figure 2 shows the fin temperature distribution for Pr=0.711,

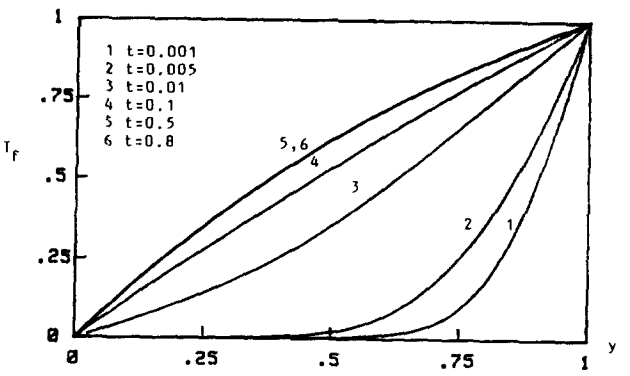

Figure 2 The temperature of the fin with Pr=0.711, Ra=8.317×10^{5}, $\alpha^{*}=4.36223$, and $k^{*}=8798.7$

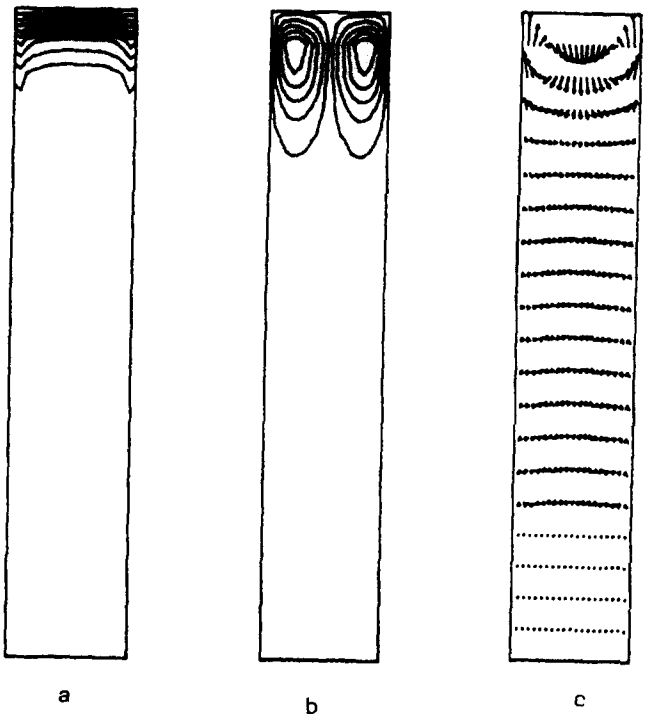

Figure 3 The fluid at $t=0.001$: (a) temperature distribution; (b) streamline; (c) velocity vector, with Pr=0.711, Ra=8.317×10^{5}, $\alpha^{*}=4.36223$, and $k^{*}=8,798.7$

Ra=8.317×10^{5}, $\alpha^{*}=4.36223$, and $k^{*}=8,798.7$. At the beginning, the fin is at initial temperature; then for $t>0$, the two ends of the fin are kept at hot and cold constant temperatures. The heat flux starts to flow into the fin, causing the fin temperature distribution to increase gradually. At $t=0.04$ the temperature reaches the cold end, and at $t=0.8$ the temperature distribution approaches the steady state.

Temperature distribution, streamline, and velocity vector of the fluid with the same parameters are shown in Figures 3–6. The fluid in the cavity is driven by the hot surface. At the beginning, the constant temperature lies are concentrated on the hot-surface region and the streamline and velocity vector form two small symmetrical vortices. Then the constant temperature lines slowly move to the cold-surface region, and the two small vortices gradually become two large symmetrical vortices. In the end, all the phenomena are approaching the steady state.

Figure 7 shows the average Nusselt number $\overline{\mathrm{Nu}}_x$ on the hot and cold wall, with fin–fluid thermal diffusivity ratios (α^{*}) of

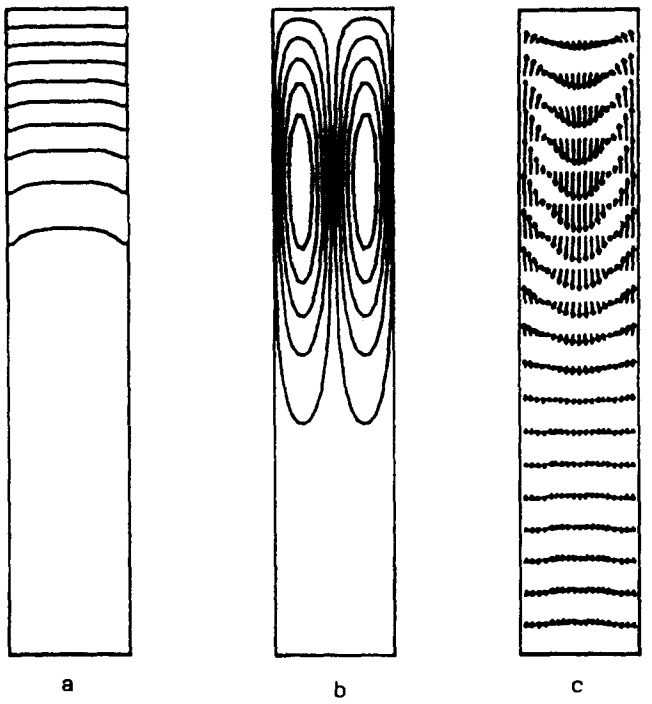

Figure 4 The fluid at $t=0.01$: (a) temperature distribution; (b) streamline; (c) velocity vector, with Pr=0.711, Ra=8.317×10^5, $\alpha^*=4.36223$, and $k^*=8{,}798.7$

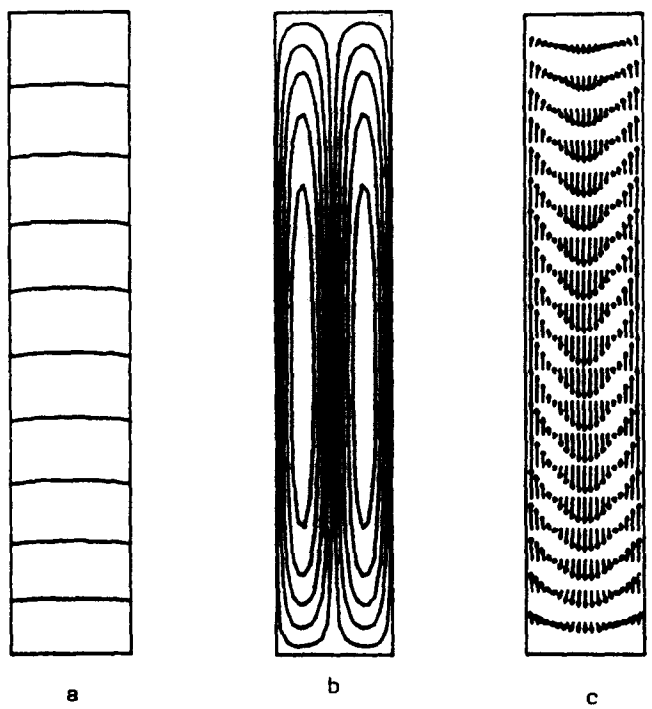

Figure 5 The fluid at $t=0.1$: (a) temperature distribution; (b) streamline; (c) velocity vector, with Pr=0.711, Ra=8.317×10^6, $\alpha^*=4.36223$, and $k^*=8{,}798.7$

4.36223 and 436.223. The average Nusselt number increases with decreasing α^* on the hot wall and decreases with decreasing α^* on the cold wall. The average Nusselt number of fin $\overline{Nu}_{fx}$ on the hot and cold wall with the same α^* has the same results (Figure 8).

Figures 9–12 indicate that the average Nusselt numbers $\overline{Nu}_x$ and $\overline{Nu}_{fx}$ are less sensitive to Ra and Pr, and $\overline{Nu}$ increases with decreasing Ra or increasing Pr on a hot wall and decreases with decreasing Ra or increasing Pr on a cold wall. Figure 13

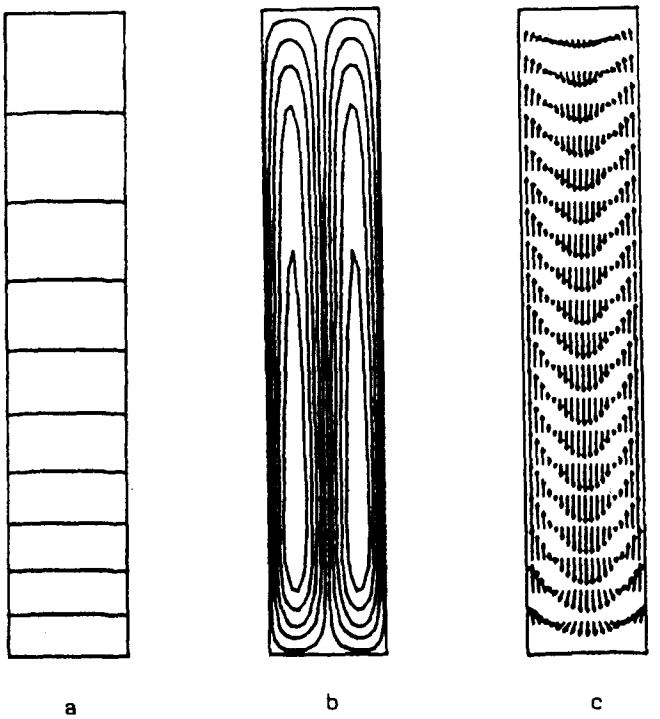

Figure 6 The fluid at $t=0.8$: (a) temperature distribution; (b) streamline; (c) velocity vector, with Pr=0.711, Ra=8.317×10^6, $\alpha^*=4.36223$, and $k^*=8{,}798.7$

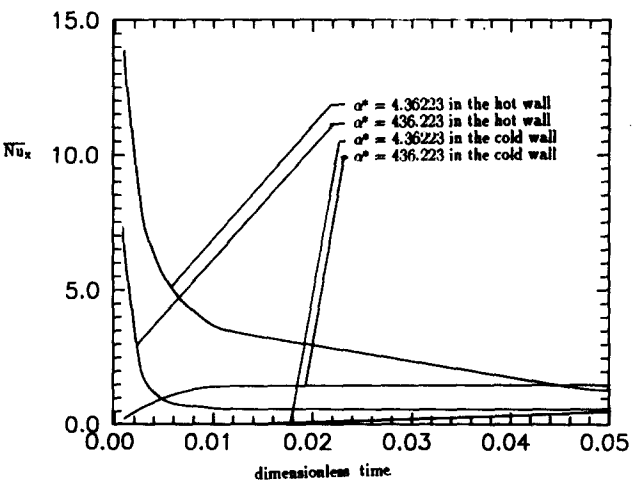

Figure 7 The average Nusselt number $\overline{Nu}_x$ on a hot and cold wall, with $\alpha^*=4.36223$ and 436.223, Pr=0.711, Ra=8.317×10^6, and $k^*=8{,}798.7$

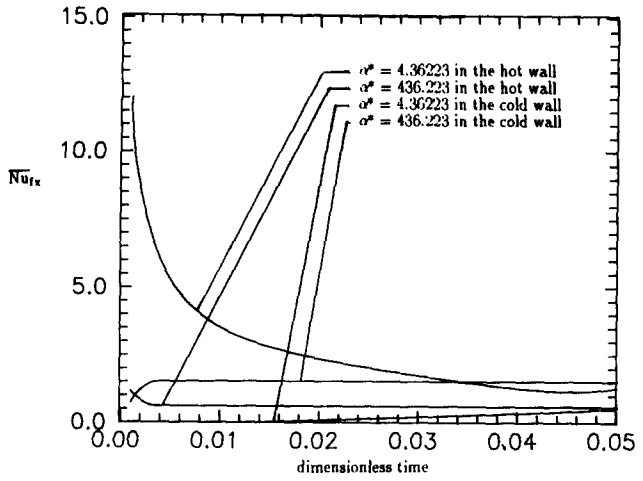

Figure 8 The average Nusselt number $\overline{Nu}_{fx}$ on a hot and cold wall, with $\alpha^* = 4.36223$ and 436.223, Pr = 0.711, Ra = 8.317×10^5, and $k^* = 8{,}798.7$

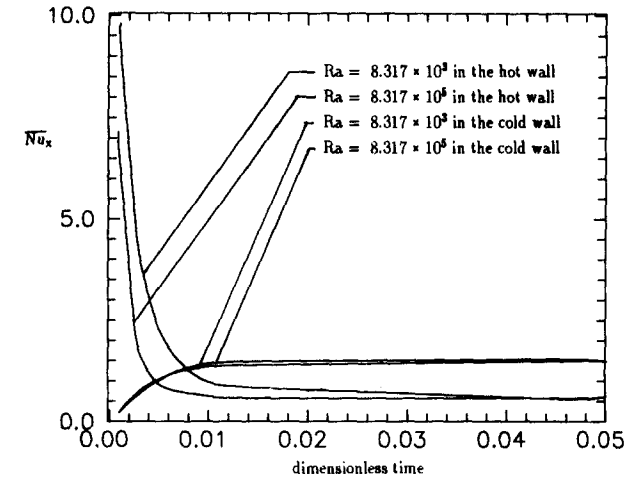

Figure 9 The average Nusselt number $\overline{Nu}_x$ on a hot and cold wall, with Ra = 8.317×10^3 and 8.317×10^5, Pr = 0.711, $\alpha^* = 436.223$, and $k^* = 8{,}798.7$

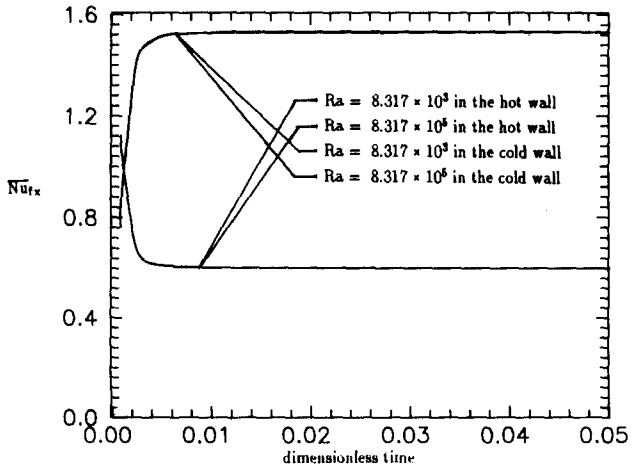

Figure 10 The average Nusselt number $\overline{Nu}_{fx}$ on a hot and cold wall, with Ra = 8.317×10^3 and 8.317×10^5, Pr = 0.711, $\alpha^* = 436.223$, and $k^* = 8{,}798.7$

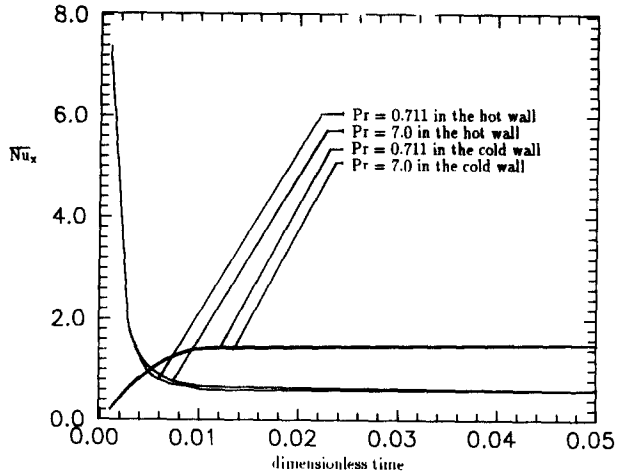

Figure 11 The average Nusselt number $\overline{Nu}_x$ on a hot and cold wall, with Pr = 0.711 and 7.0, Ra = 8.317×10^5, $\alpha^* = 436.223$, and $k^* = 8{,}798.7$

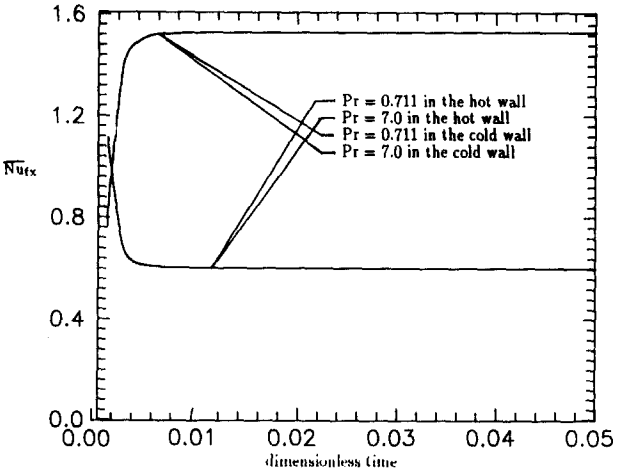

Figure 12 The average Nusselt number $\overline{Nu}_{fx}$ on a hot and cold wall, with Pr = 0.711 and 7.0, Ra = 8.317×10^5, $\alpha^* = 436.223$, and $k^* = 8{,}798.7$

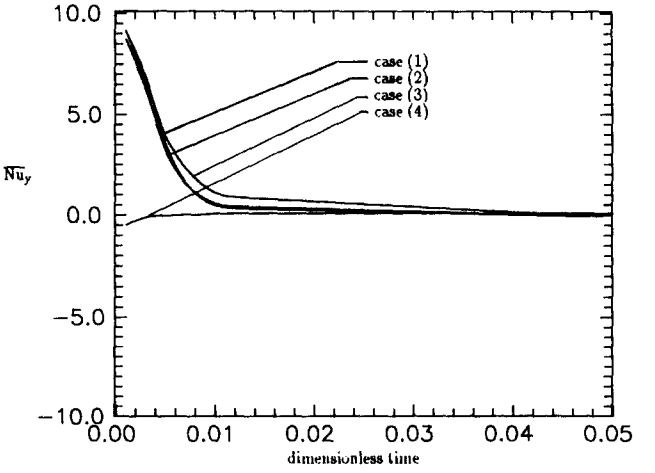

Figure 13 The average Nusselt number $\overline{Nu}_y$ on a hot and cold wall: (1) Pr = 0.711, Ra = 8.317×10^5, $\alpha^* = 436.223$, and $k^* = 8{,}798.7$; (2) Pr = 0.711, Ra = 8.317×10^3, $\alpha^* = 436.223$, and $k^* = 8{,}798.7$; (3) Pr = 7.0, Ra = 8.317×10^5, $\alpha^* = 436.223$, and $k^* = 8{,}798.7$; (4) Pr = 0.711, Ra = 8.317×10^5, $\alpha^* = 4.36223$, and $k^* = 8{,}798.7$

shows that $\overline{Nu}_y$ is also less sensitive to Ra and Pr but varies with different α^*.

Conclusions

This article presents the transient natural phenomenon of 2-D natural convection heat transfer in a rectangular cell with vertical plate fins. From the numerical results, we find that the average Nusselt numbers are less sensitive to the Raleigh and Prandtl numbers than the fin–fluid thermal diffusivity ratio.

References

1 Sparrow, E. M. and Acharya, S. A natural convection fin with a solution determined nonmontonically varying heat transfer coefficient. *J. Heat Transfer*, 1981, **103**, 218–225

2 Huang, M. J. and Chen, C. K. Vertical circular fin with conjugated natural convection–conduction flow. *J. Heat Transfer*, 1985, **107**(1), 242–245

3 Huang, M. J. and Chen, C. K. Conjugated mixed convection–conduction heat transfer along a vertical circular fin. *Int. J. Heat and Mass Transfer*, 1985, **28**(3), 523–529

4 Wang, P. and Kahawita, R. Numerical integration of partial differential equations using cubic splines. *Int. J. Computer Math.*, 1983, **13**, 271–286